

Article

Stability Assessment of Rock Slopes Using the Q-Slope Classification System: A Reliability Analysis Employing Case Studies in Ecuador

Cesar Borja Bernal ^{1,2,*}, Ricardo Laín ¹, Luis Jordá ³ , Miguel Cano ⁴ , Adrián Riquelme ⁴ 
and Roberto Tomás ⁴ 

¹ Escuela Técnica Superior de Ingenieros de Minas y Energía, Universidad Politécnica de Madrid, Calle de Ríos Rosas 21, 28003 Madrid, Spain; ricardo.lain@upm.es

² Facultad de Ciencias Naturales, Universidad de Guayaquil, Av. Raúl Gómez Lince s/n y Av. Juan Tanca Marengo, Guayaquil 090601, Ecuador

³ Department of Land Engineering and Morphology, Universidad Politécnica de Madrid, ETSICCP, Calle Profesor Aranguren 3, Campus Ciudad Universitaria, 28040 Madrid, Spain; l.jorda@upm.es

⁴ Department of Civil Engineering, University of Alicante, Carretera San Vicente del Raspeig, s/n, San Vicente del Raspeig, 03690 Alicante, Spain

* Correspondence: cesar.bbernal@alumnos.upm.es

Abstract: Q-slope is one of the most recent empirical geomechanical classification systems and the least studied in South America. This study aims to expand the knowledge base regarding the Q-slope geomechanical method and demonstrate its applicability and reliability in rock slopes of Andean countries, such as Ecuador. To this end, thirty rocky slopes have been characterized considering (1) the physical visual approach—geographic location, climate, lithology, alteration, and stability (to obtain values of Jr, Ja, Jwice, and SRFa)—and (2) geomechanical stations and kinematic analysis (for the determination of the type of failure, Jn, O-factor, and SRFc for Q-slope). Field data were collected in contrasting environments (coastal, mountain, and forest), and different failure modes were considered (planar, wedge, block, and flexural topplings) to better understand the method. The results and main contributions of this research are (i) verifying the applicability of the Jwice parameters in different climatic settings and (ii) validating the Q-slope method by applying a confusion matrix to evaluate its reliability for slope stability assessment. The overall accuracy obtained is 80%, placing the Q-slope geomechanical method in the highest evaluation quartile and thus classifying it as very good for slope characterization.

Keywords: slope stability; rock mass classifications; Andes; overall accuracy; Q-slope; reliability



Citation: Borja Bernal, C.; Laín, R.; Jordá, L.; Cano, M.; Riquelme, A.; Tomás, R. Stability Assessment of Rock Slopes Using the Q-Slope Classification System: A Reliability Analysis Employing Case Studies in Ecuador. *Appl. Sci.* **2023**, *13*, 7399. <https://doi.org/10.3390/app13137399>

Academic Editors: Pietro Mosca, Sabrina Bonetto and Chiara Caselle

Received: 19 May 2023
Revised: 12 June 2023
Accepted: 16 June 2023
Published: 22 June 2023



Copyright: © 2023 by the authors. Licensee MDPI, Basel, Switzerland. This article is an open access article distributed under the terms and conditions of the Creative Commons Attribution (CC BY) license (<https://creativecommons.org/licenses/by/4.0/>).

1. Introduction

Geomechanical classifications have been used since 1946 to characterize rock masses, mainly oriented to tunnel construction. The two most widely used geomechanical classifications are the Q-index [1] and rock mass rating (RMR) [2]. These classifications determine a quality index, estimate rock mass behavior, and provide guidelines to select the rock support measures in tunnels, open pit mines, and/or slopes [3,4]. The RMR was conceived for tunnels and adapted for foundations, open pit mining, and rock slopes and is probably the best-known and most commonly used geomechanical classification for the preliminary characterization of rock mass quality. Other classifications modify the RMR for rock slope analysis by adding correction factors such as the slope mass rating, SMR [5], initially employed for civil construction, and the mining rock mass rating, MRMR [6], used in open pit and underground mining. Although the Q-index is the leading classification system for underground design, it was not systematically applied to slopes until 2015. The Q-slope classification [7] modifies some Q-index parameters and enables the application to rock slopes. Q-slope is becoming very popular and has been applied to over 400 individual

case studies in many countries and different lithologies [8]. Nevertheless, SMR remains one of the most used geomechanical classifications for slope analysis [9,10]. SMR has been used for over 30 years, providing valuable insight into expected slope behavior. In contrast, the more recent Q-slope is an empirical rock slope engineering method used to quickly assess slope stability with minimal assumptions [11–13]. SMR and Q-slope have been successfully applied to geomechanically characterize civil construction rock slopes, global natural slopes, and quarries. However, its application and reliability in the Andean region remain relatively underexplored. The application of SMR and Q-slope in the Andean part of South America can fill a knowledge gap in terms of rock types and stability assessments on high mountain slopes.

Slope movements have become one of the most dangerous natural hazards, causing many human losses and substantial material damage annually [14]. With instabilities in rocky slopes, different methods can be used for stability evaluation. From a practical point of view, there are three main approaches to the study of rock slope failures: (a) application of geomechanical classifications and empirical analysis; (b) kinematic assessment or application of limit equilibrium methods (for block and circular failures), and (c) application of numerical methods such as finite element, finite difference, and discrete element approach. (b) and (c) present simple applications and require less information to generate reliable models; therefore, they are the most used approaches in the feasibility stages of a project.

In the study of shallow rock slopes—those without stress effects, with relatively homogeneous rock masses and heights under 50 m—limit equilibrium and kinematic are the most used methods, followed by geomechanical classifications. The Q-slope [7,8] indices can be applied to heavily fractured rock masses, presenting circular, wedge, toppling, or planar failures due to weak rock masses. Limit equilibrium methods can use slice methods and kinematic analysis. The three approaches are frequently combined in practice to study rocky slopes, with each technique providing complementary information [14,15].

Since its development in the 1970s, the Q system has been widely used in multiple projects related to civil engineering and underground mining [7]. In 2015, the empirical Q-slope method was presented, enabling technicians responsible for ongoing construction works to evaluate the stability of excavations and rock slopes as it progresses, correcting the inclination angles of the rocks in the field and profiled slopes [16]. The Q-slope index maintains the original RQD and J_n parameters of the Q-index but modifies and proposes adjustments for the J_r , J_a , and J_w factors and SRF:

- i. On slopes, the relationship of (J_r/J_a) is multiplied by a subfactor “O”, which considers the impact of discontinuity orientation on slope stability;
- ii. The J_w factor is transformed into a double parameter that analyzes the relationship between the state of the slopes and the environment in which they are located;
- iii. The SRF factor for slopes is divided into three potential lines of analysis depending on the existing field data: (a) physical condition, (b) stress, and (c) major discontinuity.

With these modifications, Q-slope values are obtained, spanning six orders of magnitude (from 0.001 to 1000) and thus determining the slope’s recommended inclination angle and failure mode [17–19].

Whether applied to tunnels, open pit mines, or slopes, the success of geomechanical classifications is based on the applicability to different scenarios that benefit from a continuously updated database of real applications. For example, the SMR classification, initially developed in 2015 for limestones, marls, and siltstones along the Spanish east coast, has been applied to many lithologies and countries. In 2015, there was evidence of SMR in over 50 countries and five continents [10].

The first publication of the Q-slope index in 2015 reported its application in Panama, Australia, Laos, and the Dominican Republic [7]. It has been since extended and applied to many other countries such as Papua New Guinea, Turkey, Serbia, Slovenia, and Spain [8].

A scientific literature review was carried out to verify the applicability of the Q-slope. The search encompassed the WOS and SCOPUS databases and included studies published until January 2022. The results detected applications of Q-slope in Australia, Norway, India,

Iran, Netherlands, Turkey, China, the United States, Spain, Italy, Algeria, the Republic of Macedonia, Brazil, Hungary, and Malawi. Besides scientific papers, the analysis included conference proceedings.

However, when focusing on the Andean slopes of Ecuador, the results confirmed a gap regarding high-impact scientific publications. The number of publications associating Ecuador and the Q-slope method is scarce. This emphasizes the relevance and necessity to validate this method in the Andean region, specifically in Ecuador, to assess its reliability. The overarching aim is to provide greater visibility to the Q-slope both in the scientific world and in applied engineering, thus contributing to regional geotectonics.

The primary aim of this study is to evaluate the applicability of the Q-slope classification in Ecuador. To this end, slopes were selected to represent the four most common types of failures: planar, wedge, flexural toppling, and block or direct toppling. The outcomes of a conventional slope kinematic analysis are used to obtain the values of some parameters employed in the equations used by the geomechanical classification [20–22]. This study also evaluates the accuracy and reliability of the Q-slope to predict real failures compared to the recommendations given by the authors of the method [7].

2. Study Sites

The Andes is a mountain range spanning from southern Chile to Colombia, in the heart of the South American continent. It is characterized by young high elevations, high plateaus, and significant slopes with deep valleys, only surpassed by the Himalayas. The roads and railways of rugged countries such as Bolivia, Peru, and Ecuador are often affected by slope failure problems. These risks entail high maintenance costs, long delays and disruptions in services, and hazards and disasters across the network of national road routes.

Ecuador is located in the northwestern corner of South America, bordering Colombia to the north, Peru to the south, and the Pacific Ocean to the west (Figure 1). The insular region of Ecuador is represented by the Galapagos Islands, named by UNESCO as a World Heritage Site, which are part of the Ecuadorian territory and the Biosphere Reserve and Ramsar Sites [23]. The present study focuses on continental Ecuador, historically marked by strong seismic events that have shaped the regional geology, dividing the country into three geological regions: (i) coast or littoral; (ii) Sierra or Interandina; and (iii) Oriente or Amazonia (Figure 1).

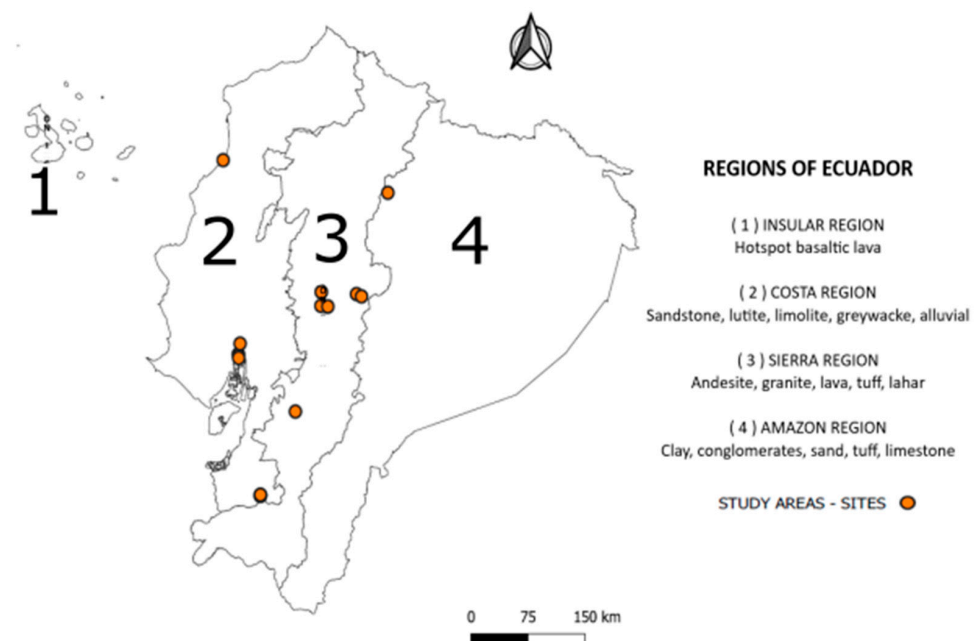


Figure 1. Geographic location of the study and geological regions of Ecuador.

The coast is subdivided into three sub-regions, south, central, and north, in which mainly sedimentary rocks are found, such as conglomerate, claystone, shale, and limestone. The Sierra is divided into north-central, central-south, and south-southwest. The predominant geology of the Sierra includes volcanic and intrusive rocks of the andesitic lavas, pyroclastic rocks, tuffs, and greywackes. The Amazon, also known as the Ecuadorian East, is divided into north, central, and south (west), with mainly sedimentary rocks such as conglomerate, sandstone, shale, claystone, gypsum, slate, and limestone. Geological materials originate from hot spots in the Galapagos Islands, with basaltic lavas dominating [24].

This section briefly lists the areas in which the studied slopes are located (Figure 1). The thirty study sites are located in seven different provinces of the three regions that constitute continental Ecuador: (i) Bellavista neighborhood, via Las Aguas and Faculty of Natural Sciences of the University of Guayaquil (Guayas province), (ii) Coaque–Santa Teresa highway (Manabí province), (iii) Vías Cahuají–Cotaló, San Juan—Guaranda and Cascada Ojo del fantasma (Chimborazo province), (iv) Papallacta road from Quito to the east (Napo province), (v) El Cajas (Azuay province), (vi) Cantera Mesa, vías Pache–Piñas and Pacha–Ayapamba (El Oro province), and (vii) vía Ambato–Guaranda, zones Cashisagua and Gallo Rumi (Bolívar province).

Guayaquil (Guayas province) is the most important city on the coast of Ecuador. Guayaquil is nestled chiefly on the banks of the Guayas River, on soft sedimentary terrain with little relief. However, to the west of Guayaquil, there is a series of hills with maximum altitudes of 300 m a.s.l., formed by folded sedimentary rocks. In this province, seven slopes (slope no. 1, 2, 3, 4, 5, 6, and 7) were studied on byways, courts, streets, and quarries. The heights of these slopes range from 4 to 18 m and include wedge, planar, and toppling stability failure types.

The Spondylus route follows the coast of Ecuador. Slope no. 8 is located in the coastal province of Manabí, on a highway called Coaque–Santa Teresa. The 12-m height slope is unstable and presents a wedge-type fault in Andesite Basalts.

The province of Chimborazo is placed in the south-central part of Ecuador and includes the Chimborazo, Tungurahua, and Altar Volcanoes as the most critical topographic features. The geology of Chimborazo is mainly composed of andesites, rhyolites, granites, lavas, volcanic tuffs, and laharitic flows. In this Andean province, five unstable and very steep Quasi-Stable slopes (slope no. 9, 10, 11, 12, and 13) are located in avenues and fairways, with heights ranging from 55 to 70 m and presenting wedge, toppling, and planar failures.

The main highway that connects the capital Quito (Sierra) to the East of Ecuador (jungle) crosses the Papallacta hot springs. This route crosscuts several basaltic lava flows of the Antisana volcano. The study slope (slope no. 14) comprises basaltic columns that project out of the road slope, causing tilting (i.e., toppling of blocks) of some columns towards the road.

The mountain pass known as El Cajas, located just 35 km from Cuenca, was declared a World Heritage Site by UNESCO. The road that connects Guayaquil to Cuenca records a 4000 m altitude difference along 120 km. The study slope (slope no. 15) within the Cajas National Park is structurally controlled and presents a typical instability of block toppling and planar failure depending on the slope area.

Piñas county is part of the El Oro (The Gold) province, named for its significant mineral deposits, actively mined since colonial times. The rocks that describe the geological system are andesitic lavas, granites, rhyolites, and slates. Six sites of interest were studied (slope no. 16, 17, 18, 19, 20, and 21), evidencing wedge failures and toppling.

The province of Bolívar extends from the slopes of the Chimborazo volcano, Arenal sector 4400 m a.s.l., to the town of Balsapamba, located 200 m a.s.l. The study areas are geologically represented by lava flows, pyroclastic rocks, laharitic flows, shales, and greywackes. Land features and accessibility to the sampling sites were the main criteria for choosing the study areas. In this province, nine slopes were surveyed, two on the Ambato–Guaranda road (slope no. 22 and 23), three in the San Juan area (slope no. 24, 25, and 26), three in the Cashisagua area (slope no. 27, 28, and 29) and one in the Gallo

Rumi area (slope no. 30). These slopes show three common failure types: planar, toppling, and wedge.

3. Materials and Methods

The proposed methodology was developed in three different phases (Figure 2): (i) field-work for data acquisition; (ii) processing of the recorded information; and (iii) validation and reliability analysis employing a confusion matrix analysis.

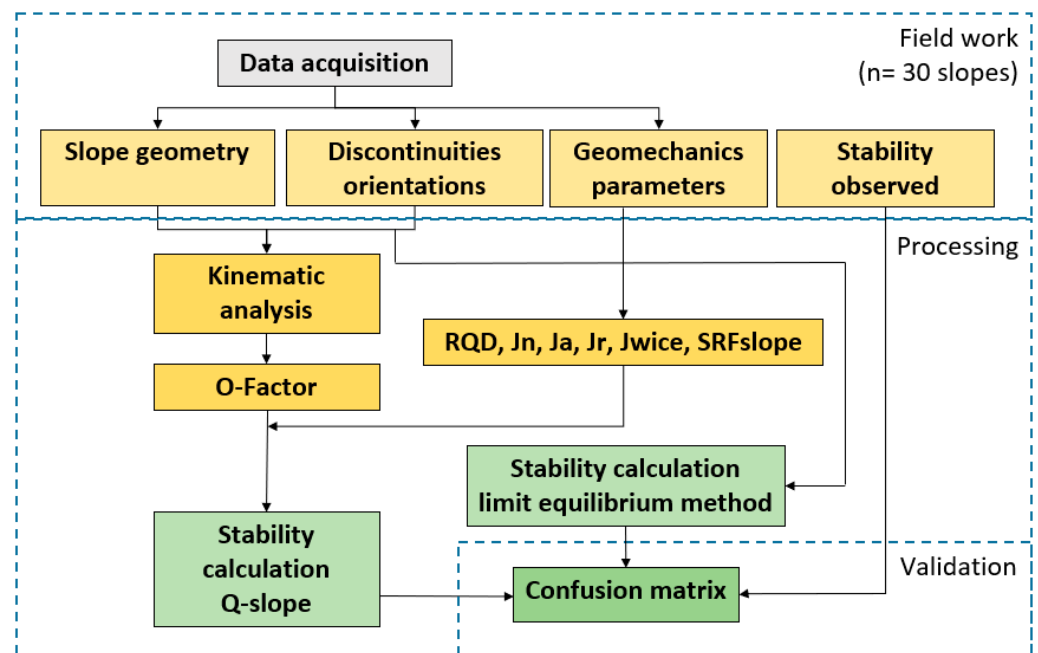


Figure 2. Scheme of the methodology followed for the application of the Q-slope method.

3.1. Data Acquisition

Fieldwork was carried out from March 2020 to January 2021. Thirty slopes were studied in seven provinces of the three continental Ecuador regions (Figures 1 and 3a). At each geotechnical survey (i.e., observation point), geometrical, physical, and structural data were collected regarding the type of rock matrix and behavior of the discontinuities that composed the bedrock (i.e., roughness, openness, persistence, and presence of water). Structural data of joints and discontinuities (dip/dip direction) were also registered, which enabled the identification of the failure for each slope. All the main types of failure were observed (i.e., wedge, toppling, and planar), with wedge failure being the most representative of the study (Figures 3 and 4). During fieldwork, slope stability was also estimated in situ as stable, almost stable, or unstable based on the signs of instability observed in the slope. Most slopes were classified as unstable at the end of the survey, while the remainder were classified as almost stable and stable.

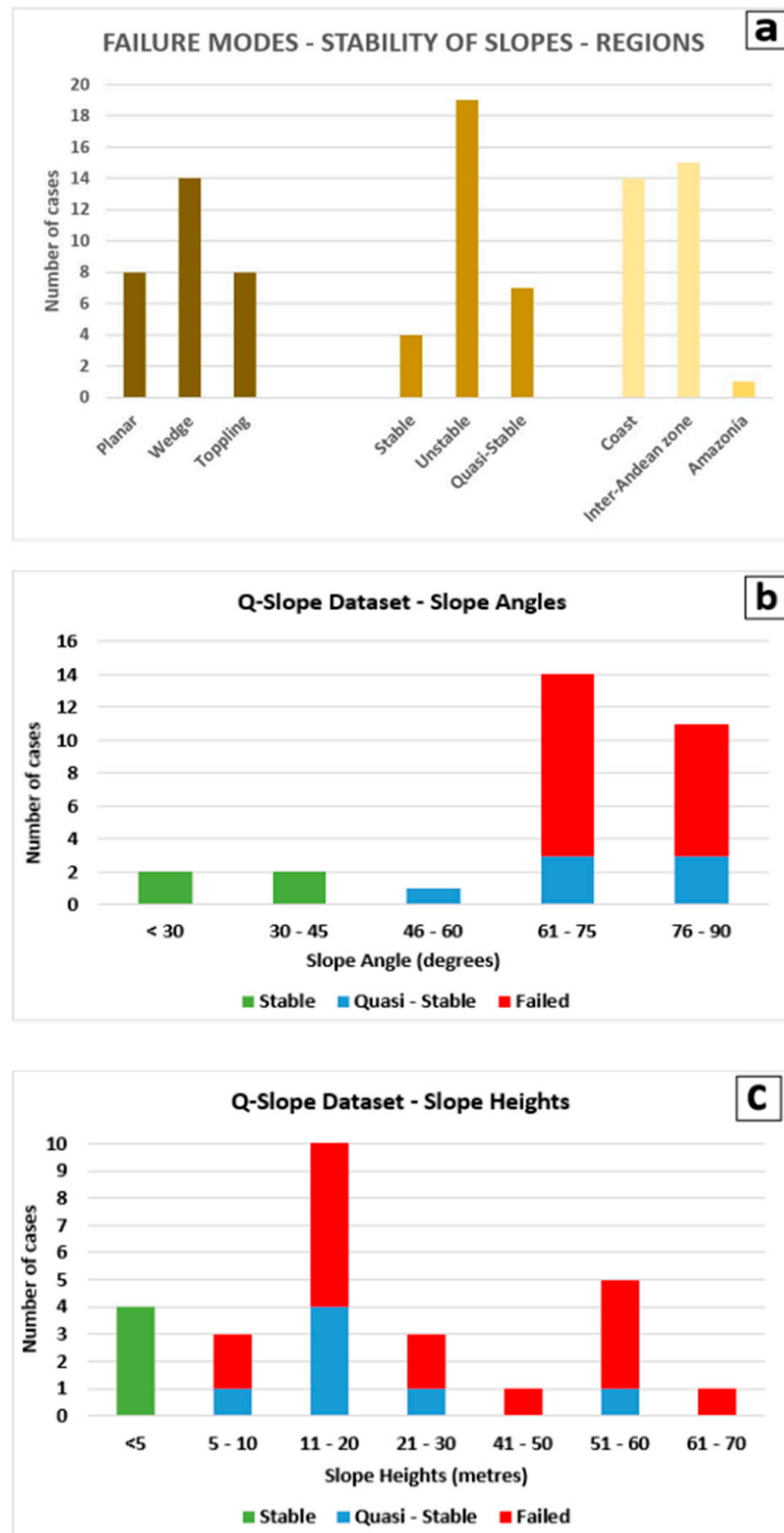


Figure 3. Case studies analyzed herein: (a) failure modes, stability, and study regions, (b) stability and slope angle, and (c) stability and height.



Figure 4. Cont.



Figure 4. Type of stability: (a) stable slope no. 2 of the School of Natural Sciences University of Guayaquil; (b) Quasi stable slope no. 22 on the Ambato-Guaranda road, slopes of the Chimborazo volcano; (c) unstable slope no. 9 of the Cahuají–Cotaló highland region road; (d) slope no. 15 in El Cajas, which presents overturning type rupture; (e) slope no. 14, in Papallacta (Ecuador), where block toppling is present in basaltic columns; (f) slope no. 5, in the Bellavista area, Guayaquil (Ecuador), which presents planar failure in siliceous siltstones; and (g) slope no. 8, in the Coaque–Santa Teresa roadway (Ecuador), which shows wedge failure in andesitic basalts.

3.2. Basic Kinematic Assessment

The analysis of wedge, planar, and block toppling failure is a tridimensional-type problem. The visualization of the interactions between discontinuity planes and slopes is exceptionally complex to analyze using isometric projection but considerably simplified with stereographic projection, in which the planes are represented by points (i.e., poles). Kinematic assessment is based on the analysis of the relative orientation of discontinuity planes or poles regarding the slope, establishing four main types of failure: (a) planar; (b) wedge; (c) flexural toppling; and (d) direct toppling [25].

Instabilities depend on the relationship between friction, the orientation of the joints, and the angle of the slope. The kinematic representation of data obtained in situ and the direct observation of evidence of instability in the slope enables a preliminary stability

assessment. This initial analysis provides a broader perspective of the problem and establishes a standard for the selection of values related to the joint set number (J_n), the favorable or unfavorable orientation of the discontinuities (O-factor), major discontinuity (SRF_c), and stable and unstable structure.

In order to assess the kinematic stability of the rock blocks, the shear strength of discontinuities is needed. In this paper, Barton's (2002) criteria for the "frictional component" of joints is used while considering the cohesion = 0 to be conservative in the design. The "Frictional Component (FC) is given by the following formula [26]:

$$FC \text{ (deg)} = \tan^{-1} \left(\frac{J_r}{J_a} \times J_w \right) \quad (1)$$

3.3. Rock Slope Quality Assessment Using Q-slope

The Q-index for slopes (or Q-slope) was conceived in 2014, mainly for an immediate application to a hydroelectric power dam in the Dominican Republic. However, the first publication on its application occurred in 2015 [7].

The equation applied to estimate the value of the Q-slope index shares two-thirds of its content with the original Q-index for underground works [7,27]. The Q-slope is calculated by Equation (2).

$$Q_{slope} = \frac{RQD}{J_n} \cdot \left(\frac{J_r}{J_a} \right)_o \cdot \frac{J_{wice}}{SRF_{slope}} \quad (2)$$

where:

RQD: Rock quality designation;

J_n : Joint set number;

J_r : Joint roughness number;

J_a : Joint alteration number;

O-factor: Orientation factor for the ratio J_r/J_a ;

J_{wice} : Environmental and geological condition number, which replaces the

Joint: water reduction factor (J_w) of the original Q-index;

SRF: Stress reduction factor for the slope. It is the maximum value between SRF_a (which addresses physical condition), SRF_b (which addresses stress, similarly to the one used in the Q-index); SRF_c: (which considers major discontinuity).

One of the novelties of the Q-slope is the discontinuity orientation factor, known as the O-Factor, which provides an adjustment to the orientation/orientations of the joints present in the studied slope [7]. This parameter is obtained after the joint kinematic analysis establishes the type of failure, considering the orientation of the main joints and the geometry of the slope. The O-Factor is determined from a table in which the only information required is whether the joint (planar failure) or joints (in the case of wedge failure) are very favorably oriented, quite favorable, unfavorable, very unfavorable, or causing failure if unsupported [8]. The information required to identify the O-Factor is easily obtained from the preliminary kinematic analysis of the study cases and field data.

Another parameter of interest is the strength reduction factor (SRF), which is relevant to consider when the quality of the materials constituting the rocky mass is not high and the heights of the slope increase. These singularities require the appropriate study of the strength state [8]. The strength reduction factor is estimated from the most unfavorable value recorded for subfactors SRF_a, physical condition; SRF_b, which analyzes various stress–strength ranges; and SRF_c, major discontinuity. These subfactors are calculated from data on the type of excavation, blasting, susceptibility to weathering, the physical state of the blocks that constitute the slope, erosion state, unconfined compressive strength, the physical state of the major discontinuity, RQD, and maximum main strength. Depending on available data on sub-parameters a, b, and c, the authors suggest selecting the most unfavorable value or discarding one of the complementary sub-values and only considering

the one with the most reliable information that allows for the selection of the best value for SRF.

For further details about the description and pondering of each factor, the reader is referred to [7,28].

The authors of method [7] also proposed the maximum stable angle of the slope (β), expressed in sexagesimal degrees, for a given Q-slope value (Equation (3)).

$$\beta = 20 \log_{10} Q_{slope} + 65^\circ \quad (3)$$

The geomechanical Q-slope classification requires information on the impact of the construction method on the slope, the state of the surroundings, and effects on exposed slopes, considering the weather, water effects, ice, and evidence of material transportation by gravitational force. Evidence of constructive methods and environmental state was carefully surveyed and compared with the back-analysis of variables—this procedure minimized significant errors in the final evaluation.

3.4. Calculation of the Factor of Safety

The factor of safety is calculated from kinematic analysis using limit equilibrium methods. RocPlane and RocTopple software from Rocscience are used for the evaluation of the stability of planar and toppling failures, respectively. Similarly, the freeware Orwa is used for the case of wedges [29,30]. The factor of safety (FoS) is then calculated for each slope in a deterministic mode, which is representative of the actual state of the study slopes.

3.5. Validation and Reliability of the Results (Confusion Matrix)

A confusion matrix is a tool employed to assess the errors of a classification system [31,32].

A statistical methodology of multivariate data was used to validate the study method, which compares the information obtained in situ against data calculated by software and the classification method. In the case study presented herein, data on the estimated or observed stability of slopes were compared with the information calculated by the empirical Q-slope method and factor of safety (FoS) obtained with software through a confusion or error matrix [33].

The first step in developing a confusion matrix is to classify obtained data as true positives and true negatives or false positives and false negatives. This was accomplished for the sub-classes stable, quasi-stable, and failed. The later calculation of the truth overall and classification overall of each class required the horizontal and vertical sums of the data classified in step one.

The percentage value of user accuracy—recall (UA) and producer accuracy—precision (PA) is the ratio between the true positive values of each analyzed class and the values obtained in step one for truth overall and classification overall, respectively (Equations (4) and (5)).

$$UA \text{ (recall)} = \frac{\text{True positive}}{\text{Truth overall}} \quad (4)$$

$$PA \text{ (precision)} = \frac{\text{True positive}}{\text{Classification overall}} \quad (5)$$

Finally, the overall accuracy (OA) is calculated from the sum of all true positive values of all variables, divided by the amount (n) of samples analyzed (Equation (6)). The overall error of the method is obtained from the difference between the maximum OA value possible and the value calculated by the confusion matrix for the same parameter.

$$OA = \frac{\Sigma \text{ True positive (class Stable, Quasi – stable and Failed)}}{n} \quad (6)$$

4. Results

Figure 3 shows the Q-slope dataset (case studies) of the failure modes, stability study regions of the analyzed slopes, and the distribution of slope angles and heights. Based on the slope’s stability and inclination angle, these are considered stable up to 45° (Figure 3b). Beyond 45°, the slopes can be almost stable or unstable. From 61° to 90°, slopes classified as unstable appear and persist with their maximum peak in the inclination range of 61° to 75° (Figure 3b). The comparative analysis between slope stability and height determined that slopes under five meters are stable. The “almost stable” definition disappeared in height ranges 41–50 m and 61–70 m. The slope failures started at 5 m and were present in all analyzed ranges, with maximum values in the 11–20 m and 51–60 m intervals (Figure 3c).

Slopes were analyzed in different climatic conditions, including locations exposed to powerful elements such as water, ice, and gravity. Interestingly, almost all the values proposed by the authors [7] for Jwice were selected. In the paper, the degree of fracturing of the RQD/Jn rock mass, condition of the discontinuities (Jr/Ja), stability, and geological and environmental factors are analyzed and presented (Tables 1 and 2).

The Q-slope calculations for each slope are summarized in Table 1 and plotted in Figure 5, as proposed by Barton and Bar [8]. The plot shows three areas: zone of stable slopes, zone of unstable slopes, and zone of almost stable slopes (i.e., slopes with uncertain stability or when it is challenging to predict slope behavior). The slope angle and Q-slope values were plotted to locate the studied slopes in the Barton and Bar graph. Four slopes were identified in the stable zone, one in the uncertainty zone, and the remainder in the unstable zone.

A confusion matrix enables a fast and easy visualization of the performance of a classification model. In a confusion matrix, the results obtained are displayed in rows and columns representing, respectively, the number of predictions of each class and the occurrences of the observed class. Three assessment sub-categories were assigned for the observed and predicted classes calculated by the Q-slope method and for the predicted class calculated with software to obtain the factor of safety (FoS): stable slopes = sub-class 1, quasi-stable = sub-class 2, and unstable or failed sloped = sub-class 3 (Table 3). A comparison of classes yields true positive, false positive, and false negative values required for calculating metrics. In this study, three confusion matrices were employed (or three analyses) to predict how the empirical method can effectively classify 30 rock slopes by comparing calculated and empirical values, data gathered in situ through direct observation, and the values calculated by software Orwa, Rocplane, and Roctopple.

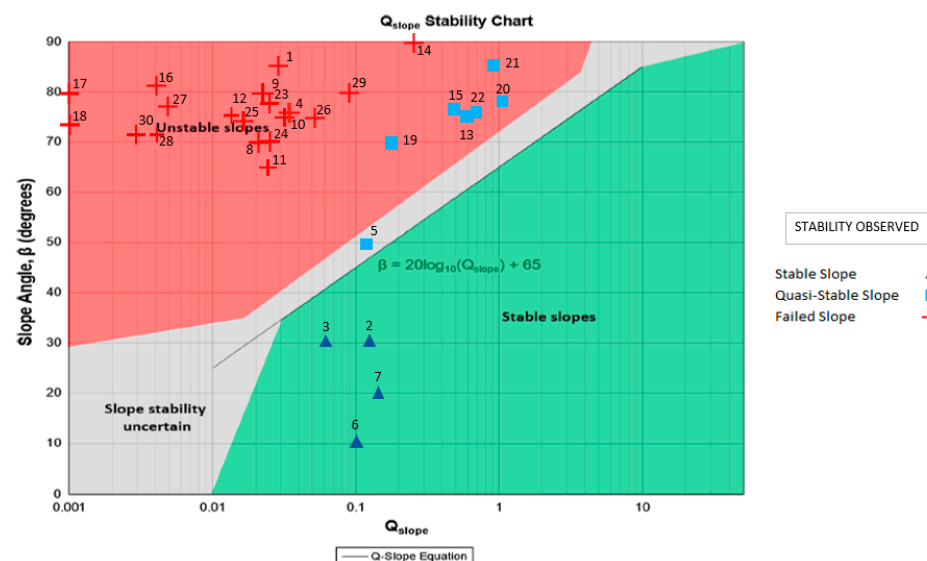


Figure 5. Q-slope data of the 30 analyzed slopes plotted over the slope angle and rock mass quality chart proposed by Barton and Bar (2017). Refer to Table 1 for more details on the slopes.

Table 1. Q-slope values, geomechanical parameters, location, characteristics, and stability of the analyzed slopes (* drainage measures installed).

No.	Zone of Ecuador	Province of Ecuador	Location	Use	Height in Meters	Slope Angle in Degrees	Q-Slope Value Calculation Factors					Stability Observed	Failure Mode	
							RQD	Jn	(Jr/Ja)o	Jwice	SRF Slope			Q-slope Value
1	Coast	Guayas	F. CC NN 1	Byway	10	85	70	9	0.759	0.05	10	0.030	Unstable	Wedge
2	Coast	Guayas	F. CC NN 2	Court	4	30	75	12	0.750	0.3	10	0.141	Stable	Planar
3	Coast	Guayas	F. CC NN 3	Street	4	30	65	12	0.375	0.3	10	0.061	Stable	Toppling
4	Coast	Guayas	Las Aguas *	Street	15	75	90	12	0.563	0.075	10	0.032	Unstable	Toppling
5	Coast	Guayas	Bellavista	Street	18	50	60	15	0.375	0.7	8	0.131	Q-stable	Planar
6	Coast	Guayas	Santa Rosa	Quarry	2	10	98	12	0.375	0.5	15	0.102	Stable	Toppling
7	Coast	Guayas	Santa Rosa	Quarry	3	20	99	12	0.375	0.5	10	0.155	Stable	Toppling
8	Coast	Manabí	Coaque–S.Teresa	Avenue	12	70	80	15	0.044	0.7	8	0.020	Unstable	Wedge
9	Andean	Chimborazo	Cahuaji–Cotaló 1	Avenue	60	80	90	15	0.075	0.5	10	0.023	Unstable	Wedge
10	Andean	Chimborazo	Cahuaji–Cotaló 2	Avenue	55	75	90	12	0.083	0.5	10	0.031	Unstable	Planar
11	Andean	Chimborazo	Cahuaji–Cotaló 3	Avenue	60	65	95	12	0.063	0.5	10	0.025	Unstable	Wedge
12	Andean	Chimborazo	Cahuaji–Cotaló 4	Avenue	70	75	95	12	0.038	0.5	10	0.015	Unstable	Wedge
13	Andean	Chimborazo	Cascada	Fairway	60	75	95	12	0.563	0.7	5	0.623	Q-stable	Planar
14	Amazon	Napo	Papallacta	Avenue	18	90	90	15	0.380	0.6	5	0.270	Unstable	Toppling
15	Andean	Azuay	El Cajas	Avenue	13	77	100	9	0.380	0.6	5	0.500	Q-stable	Planar
16	Coast	El Oro	La Mesa 1	Quarry	50	82	75	15	0.150	0.05	10	0.004	Unstable	Toppling
17	Coast	El Oro	La Mesa 2	Quarry	60	80	30	12	0.056	0.05	10	0.001	Unstable	Wedge
18	Coast	El Oro	La Mesa 3	Quarry	25	74	55	15	0.100	0.05	15	0.001	Unstable	Toppling
19	Coast	El Oro	Pache–Piñas	Avenue	17	70	100	12	0.380	0.3	5	0.190	Q-stable	Wedge
20	Coast	El Oro	Pacha–Ayapamba 1	Avenue	15	78	85	15	6.075	0.3	10	1.033	Q-stable	Wedge
21	Coast	El Oro	Pacha–Ayapamba 2	Avenue	25	85	80	15	6.075	0.3	10	0.972	Q-stable	Wedge
22	Andean	Bolívar	Ambato–Guaranda 1	Highway	10	75	95	9	0.750	0.9	10	0.713	Q-stable	Planar
23	Andean	Bolívar	Ambato–Guaranda 2	Highway	18	77	65	15	0.083	0.7	10	0.025	Unstable	Planar
24	Andean	Bolívar	San Juan 1	Avenue	15	70	60	12	0.169	0.3	10	0.025	Unstable	Wedge
25	Andean	Bolívar	San Juan 2	Avenue	10	75	80	12	0.125	0.2	10	0.017	Unstable	Toppling
26	Andean	Bolívar	San Juan 3	Avenue	12	75	90	12	0.225	0.3	10	0.051	Unstable	Wedge
27	Andean	Bolívar	Cashisagua 1	Avenue	17	77	80	12	0.025	0.3	10	0.005	Unstable	Wedge
28	Andean	Bolívar	Cashisagua 2	Avenue	20	72	85	12	0.019	0.3	10	0.004	Unstable	Wedge
29	Andean	Bolívar	Cashisagua 3	Avenue	30	80	95	12	0.375	0.3	10	0.089	Unstable	Planar
30	Andean	Bolívar	Gallo Rumi	Avenue	12	72	50	15	0.050	0.2	10	0.003	Unstable	Wedge

Table 2. Kinematic assessment of the studied rock slopes.

No.	Zone of Ecuador	Slope Dip	Slope Dip Direction DipDir	Failure Mode	Joint DipDir	Joint Dip	Joint 2 DipDir (Wedges)	Frictional Component FC (Degrees)	Factor of Safety FS	Stability Factor of Safety
1	Coast	85	060	Wedge	072	65	023	48	0.27	Unstable
2	Coast	30	035	Planar	030	73		37	>1	Stable
3	Coast	30	215	Toppling	192	16		37	>2	Stable
4	Coast	75	180	Toppling	187	15		37	>3	Stable
5	Coast	50	192	Planar	180	44		30	0.6	Unstable
6	Coast	10	208	Toppling	203	17		21	>1	Stable
7	Coast	20	345	Toppling	336	34		21	>2	Stable
8	Coast	70	110	Wedge	034	60	140	30	0.73	Unstable
9	Andean	80	090	Wedge	155	77	077	11	0.25	Unstable
10	Andean	75	095	Planar	108	77		25	>1	Stable
11	Andean	65	090	Wedge	034	62	117	30	0.61	Unstable
12	Andean	75	115	Wedge	151	61	048	30	0.51	Unstable
13	Andean	75	180	Planar	186	49		37	0.5	Unstable
14	Amazon	90	210	Toppling	065	80		30	0.23	Unstable
15	Andean	77	161	Planar	175	31		32	>1	Stable
16	Coast	82	050	Toppling	056	82		11	0.33	Unstable
17	Coast	80	325	Wedge	289	88	038	5	0.77	Unstable
18	Coast	74	272	Toppling	272	78		11	0.58	Unstable
19	Coast	70	126	Wedge	203	85	105	29	>1	Stable
20	Coast	78	137	Wedge	163	71	063	32	0.4	Unstable
21	Coast	85	145	Wedge	139	84	184	30	0.31	Unstable
22	Andean	75	060	Planar	062	79		37	>1	Stable
23	Andean	77	120	Planar	105	76		9	0.14	Unstable
24	Andean	70	040	Wedge	345	43	272	14	0.62	Unstable
25	Andean	75	020	Toppling	010	63		14	0.59	Unstable
26	Andean	75	028	Wedge	113	44	004	40	0.83	Unstable
27–28	Andean	72	005	Wedge	309	71	009	20	0.33	Unstable
29	Andean	80	080	Planar	099	77		37	0.13	Unstable
30	Andean	72	015	wedge	310	77	093	7	1.16	Stable

Statistical analysis of data revealed that of the 30 values obtained in the field (observed class), processed by the Q-slope method and processed by software (predicted class) according to the stable, almost stable, and failure sub-classes:

- For statistical study cases a and b, 24 values are true positive values, and only 6 were classified as false positives–negatives; for statistical case c, 21 are true positive values, and 9 cases were classified as false positives–negatives.
- For case a, a 100% value was obtained in producer accuracy (precision) with the stable and quasi-stable classes–the remaining sub-classes and statistical cases produced 95% and lower values.
- Regarding user accuracy (recall), 100% values were obtained for all statistical cases with sub-class stable. Case a with sub-class failed also produced a 100% value. Other sub-classes and statistical cases registered values of 89% and lower.
- The overall accuracy parameter, which defines the quality of the result obtained for the classification method (Guan et al., 2020), provided an 80% value for statistical cases a and b and 70% for case c.

Considering that the number of stable, quasi-stable, and unstable slopes is random and that the distribution of sub-class values in the confusion matrix is not homogeneous, the metric F1 score was selected as it summarizes effectively in a single value the precision and recall of the method [34].

Table 3. Results of the confusion matrices for the three statistical study cases, considering data observed in the field, calculated with Q-slope and calculated with software (Factor of safety-FoS).

Statistical Case a: Predicted Class (Q-slope) Compared to Observed Class							
Sub-Class	n (Truth Overall)	n (Classified)	Accuracy	Precision	Recall	F1 Score	Overall Accuracy
1	4	4	100%	1.00	1.00	1.00	80%
2	7	1	80%	1.00	0.14	0.25	
3	19	25	80%	0.76	1.00	0.86	
Statistical Case b: Predicted Class (FoS) Compared to Predicted Class (Q-slope)							
Sub-Class	n (Truth Overall)	n (Classified)	Accuracy	Precision	Recall	F1 Score	Overall Accuracy
1	4	9	83.33%	0.44	1.00	0.62	80%
2	1	0	96.67%	0.00	0.00	0.00	
3	25	21	80.00%	0.95	0.80	0.87	
Statistical Case c: Predicted Class (FoS) Compared to Observed Class							
Sub-Class	n (Truth Overall)	n (Classified)	Accuracy	Precision	Recall	F1 Score	Overall Accuracy
1	4	9	83.33%	0.44	1.00	0.62	70%
2	7	0	76.67%	0.00	0.00	0.00	
3	19	21	80.00%	0.81	0.89	0.85	

5. Discussion

There is a clear correlation between slopes visualized as stable and those calculated as stable using the Q-slope. Slope no. 2, 3, 6, and 7, classified as “stable”, are also classified as “stable” according to the graph proposed in 2017 for the Q-slope. It should be mentioned that slope no. 2 and 3 have been controlled for seven consecutive years because of their geographical location and access, exhibiting no evidence of instability during the monitoring period. Slope no. 5 was classified in the field as “not very stable” and is in the zone of “Quasi-Stable” slopes in the Q-slope graph [8].

However, for the remaining 25 slopes, there are slight differences between what is predicted by the Q-slope method and what is observed. Slope no. 13, 15, 19, 20, 21, and 22 were classified in the field as “Quasi-Stable”. However, they were located in the “unstable slope” graph area. The original graph [8] seems conservative and on the safe side for these slopes (Figure 6), which is very reasonable for empirical and pre-design analysis.

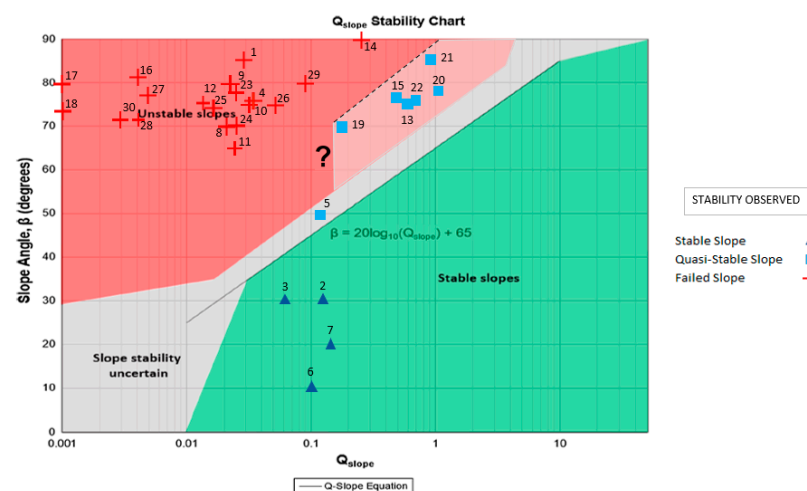


Figure 6. Modification proposal for limit lines separating stability categories. Plotted over the slope-angle and rock mass quality chart proposed by Barton and Bar (2017) with the results from Figure 5.

Considering the data obtained for slopes 13, 15, 19, 20, 21, and 22 in the present work, an extension to the area of “Slope stability uncertain” is proposed, and the door is also left open for new studies to determine the possible projection from the proposed area towards the lower part of the “Unstable slopes–slope stability un-certain” zone. The kinematic analysis does not consider rock mass quality but analyzes the equilibrium of rigid blocks that destabilize through one or more surfaces and slip on each other. In the 30 analyzed cases, failures occurred through discontinuities, and kinematic analysis was the best representation of reality. Although the friction angle and joint directions are not considered in the equation proposed by Barton and Bar (2015) (Equation (1)), these are necessary to validate the faults identified in situ, related to joint orientation and how slope faults are produced. This analysis enables the selection of a suitable O-factor, essential for Q-slope calculation. Based on the kinematic analysis, the amount of joint sets present can be ratified, and therefore, the value of J_n that represents the analyzed slope can be defined.

The main issue encountered when using the Q-slope index is the precise determination of the O-factor in those slopes affected by toppling failures. In addition, this O-factor is highly biased when quantifying slopes affected by toppling ruptures. The authors of the Q-slope method determined that applying the O-factor to toppling cases could consider the same criteria of planar and wedge cases. Still, in flexural and block toppling, the discontinuity and intersections dip inside the bedrock (180° more than direct planar failure). This suggests a revision is required when applying the O-factor to toppling (in Q-slope). With flexural toppling failure, there is just one joint set to be considered (as in planar failure), but the critical factor is slightly different. Direct or block toppling is infrequent because it involves three joint sets, of which two present an intersection dipping inwards between the rock mass and the basal plane. Regarding block toppling failure, the O-factor should consider the intersection pole of the two planes that delimit the corner. This intersection must dip towards the mountain. The O-factor should also consider the basal joint of the block in a similar approach to the kinematic assessment of planar failure. However, obtaining an O-factor value from the corner intersection or basal joint analyses is not recommended.

This research indirectly validates the J_{wice} and SRFa parameters by providing data collected at different altitudes or extreme topographic zones in very humid tropical and high mountain environments with ice. The results emphasize the need to determine the quality of the rock and the stress to which it is subjected (J_{wice} and SRFb parameters) when calculating the Q-slope. A relevant contribution presented herein is the statistical reliability assessment based on a confusion matrix to establish Q-slope’s individual and general predictive precision, providing high metrics.

The analysis of the results obtained from the confusion matrix indicates that data confusion can be attributed to the current threshold for quasi-stable slopes in the Q-slope graph proposed by Barton and Bar in 2015. This zone presents conservative (considering safety) values between Q-slope values of 0.02 and 0.4 and slope angles between 35 and 84 on the Q-slope stability graph. This singularity in the Q-slope graph requires further research that enables the zone's broadening, as proposed by Jorda [19]. It must be highlighted that the six slopes that were not classified as quasi-stable by the Q-slope method and do not present evident field instability processes are located very close to the area of uncertain stability proposed by the authors of the method in 2015. The potential broadening of the zone of quasi-stable slopes would improve the confusion matrix metrics presented in this study, obtaining future results in favor of the empirical method studied herein.

6. Conclusions

Rock mass classifications have been successfully used worldwide for rock slope characterization for multiple reasons: effectiveness due to their connection with empirical methods and dissemination and communication across scientists, engineers, and the general public. In other words, rock mass classifications “put numbers to geology” [35]. The Q-slope method was applied herein in three natural regions of Ecuador—coast, mountains, and jungle—where igneous, sedimentary, and metamorphic rocks exhibiting different weathering conditions were found.

The result of the stability analysis using the Q-slope method determined that of the 30 slopes analyzed, 25 are in unstable conditions, 1 is almost stable, and 4 slopes are in stable conditions. The results demonstrated that instability processes occur for slopes starting at 61 degrees of inclination and 6 m high.

One of the main modifications implemented in the Q-method for its application to slopes is the shear strength, which, in our specific case, is obtained by multiplying the J_r/J_a ratio by the new O-factor. Nevertheless, when slopes that present toppling failures are studied, the method does not clearly establish the values to be considered for the O-factor (differently from the cases of planar and wedge failures). Therefore, future investigation is advisable to determine the O-factor values rigorously and accurately, especially for the toppling cases. The parameter could depend on the difference in strikes and dips between slope and joints, following the determination of the F1, F2, and F3 factors of the SMR correction.

Considering the values obtained and the metrics calculated for each class of statistical case a, it can be concluded that as sub-class 1 presents high values for precision and recall, the method can perfectly classify this sub-class. For sub-class 2, a high precision value is obtained with a low recall value; in this case, the method does not classify this class very well—however, when it does, it is highly reliable. For sub-class 3, the model provides a low precision value and a high recall value, which suggests that the method classifies the sub-class well but can also confuse the individuals of other sub-classes. The F1 score values obtained for each sub-class in the different statistical cases analyzed present values that range from 0.62 to 1, indicating that the Q-slope method is a balanced method that can confuse some cases as false but is also capable of correctly classifying all positive true cases, such as those of sub-class 1 of statistical case a. Only sub-class 2 of statistical case a returned an F1 score value of 0.25, which means that the model can confuse values as false for this specific case. Sub-classes 2 for statistical cases b and c present null values because the calculated FoS is a fixed value that only defines if the slope is stable or unstable. In these cases, a direct association could not be made between the quasi-stability obtained in situ and that predicted by the empirical method and FoS.

In general, considering that overall accuracy can be divided into quartiles, classifying quartile C1 as bad, C2 as intermediate, C3 as good, and C4 as very good, the value obtained for OA herein occupies the highest quartile, ranking the method as very good.

The results demonstrated the applicability and reliability of the Q-slope method in Ecuador. This Andean country can be considered a natural laboratory for geosciences because of its diversity in geological, geomorphological, and environmental conditions.

Author Contributions: Conceptualization, C.B.B., L.J. and R.L.; methodology, C.B.B. and L.J.; validation, C.B.B., L.J., R.L., R.T., M.C. and A.R.; formal analysis, L.J., R.T. and C.B.B.; investigation, C.B.B., L.J. and R.L.; writing—original draft preparation, C.B.B., L.J., R.L., R.T., M.C. and A.R.; writing—review and editing, C.B.B. and L.J.; supervision, C.B.B., L.J., R.L., R.T., M.C. and A.R. All authors have read and agreed to the published version of the manuscript.

Funding: This work was partially funded by the University of Alicante (vigrob-157 project), the Prometheus Project of the Secretariat of Higher Education, Science, Technology and Innovation of the Republic of Ecuador (for field data acquisition from 2014 to 2015), FCI Projects at the Faculty of Natural Sciences of University of Guayaquil, and by Conselleria de Innovación, Universidades, Ciencia y Sociedad Digital in the framework of the project CIAICO/2021/335.

Institutional Review Board Statement: Not applicable.

Informed Consent Statement: Not applicable.

Data Availability Statement: Not applicable.

Acknowledgments: The authors are grateful to Roberto Chan and Marlon Cabrera at ESPOL for their assistance in gathering data along the Guayaquil slope. Thanks are extended to Rafael Jordá (Rudnik engineers, S.L.) and Ximena Robles for their collaboration in Coaque and Papallacta, respectively. Special thanks are given to RocscienceEducation version at ESPOL and the MSc and Ph.D. Students.

Conflicts of Interest: The authors declare no conflict of interest.

References

1. Barton, N.; Lien, R.; Lunde, J. Engineering Classification of Rock Masses for the Design of Tunnel Support. *Rock Mech.* **1974**, *6*, 189–236. [CrossRef]
2. Bieniawski, Z.T. Engineering rock mass classifications: A complete manual for engineers and geologists in mining, civil, and petroleum engineering. In *Engineering Rock Mass Classifications: A Complete Manual for Engineers and Geologists in Mining, Civil, and Petroleum Engineering*; Wiley: Hoboken, NJ, USA, 1989.
3. Pantelidis, L. Rock slope stability assessment through rock mass classification systems. *Int. J. Rock Mech. Min. Sci.* **2009**, *46*, 315–325. [CrossRef]
4. Moon, V.; Russell, G.; Stewart, M. The value of rock mass classification systems for weak rock masses: A case example from Huntly, New Zealand. *Eng. Geol.* **2001**, *61*, 53–67. [CrossRef]
5. Romana, M. New adjustment ratings for application of Bieniawski classification to slopes. In Proceedings of the International Symposium on Role of Rock Mechanics, Zacatecas, Mexico, 2–4 September 1985; pp. 49–53. Available online: [https://www.scrip.org/\(S\(351jmbntvnsjt1aadkposzje\)\)/reference/ReferencesPapers.aspx?ReferenceID=253061](https://www.scrip.org/(S(351jmbntvnsjt1aadkposzje))/reference/ReferencesPapers.aspx?ReferenceID=253061) (accessed on 16 July 2022).
6. Laubscher, D.H. Geomechanics classification system for the rating of rock mass in mine design. *J. S. Afr. Inst. Min. Metall.* **1990**, *90*, 257–273. [CrossRef]
7. Barton, N.; Bar, N. Introducing the Q-slope method and its intended use within civil and mining engineering projects. In Proceedings of the ISRM Regional Symposium, EUROCK 2015, Salzburg, Austria, 7–10 October 2015; pp. 157–162.
8. Bar, N.; Barton, N. The Q-Slope Method for Rock Slope Engineering. *Rock Mech. Rock Eng.* **2017**, *50*, 3307–3322. [CrossRef]
9. Romana, M.; Tomás, R.; Serón, J.B. Slope Mass Rating (SMR) geomechanics classification: Thirty years review. In Proceedings of the 13th ISRM International Congress of Rock Mechanics, Montreal, Canada, 10–13 May 2015; pp. 1–10.
10. Tomás, R.; Romana, M.; Serón Gáñez, J.B. Review of the Current Status of the Geomechanics Classification Slope Mass Rating (SMR). *Bol. Soc. Española Mecánica Suelos Ingeniería Geotécnica* **2017**, *190*, 25–32. Available online: <http://rua.ua.es/dspace/handle/10045/70953> (accessed on 20 September 2022).
11. Azarafza, M.; Nanekaran, Y.A.; Rajabion, L.; Akgün, H.; Rahnamarad, J.; Derakhshani, R.; Raoof, A. Application of the modified Q-slope classification system for sedimentary rock slope stability assessment in Iran. *Eng. Geol.* **2020**, *264*, 105349. [CrossRef]
12. Siddique, T.; Pradhan, S.P.; Vishal, V.; Singh, T.N. Applicability of Q-slope Method in the Himalayan Road Cut Rock Slopes and Its Comparison with CSMR. *Rock Mech. Rock Eng.* **2020**, *53*, 4509–4522. [CrossRef]
13. Yellaz, C.; Benzaid, R.; Tekkouk, M. Application of classification systems for the assessment of rock mass stability—Case of national road 43, Jijel, Algeria. *Arab. J. Geosci.* **2021**, *14*, 203. [CrossRef]
14. Umrao, R.K.; Singh, R.; Ahmad, M.; Singh, T.N. Stability Analysis of Cut Slopes Using Continuous Slope Mass Rating and Kinematic Analysis in Rudraprayag District, Uttarakhand. *Geomaterials* **2011**, *1*, 79–87. [CrossRef]

15. Siddique, T.; Masroor Alam, M.; Mondal, M.E.A.; Vishal, V. Slope mass rating and kinematic analysis of slopes along the national highway-58 near Jonk, Rishikesh, India. *J. Rock Mech. Geotech. Eng.* **2015**, *7*, 600–606. [[CrossRef](#)]
16. Bar, N.; Barton, N.R. Empirical slope design for hard and soft rocks using Q-slope. In Proceedings of the 50th US Rock Mechanics/Geomechanics Symposium, Houston, TX, USA, 26–29 June 2016; Volume 2, pp. 1301–1308.
17. Bar, N.; Barton, N. Q-slope: An empirical rock slope engineering approach in Australia. *Aust. Geomech. J.* **2018**, *53*, 73–86.
18. Bar, N.; Barton, N. Rock slope design using q-slope and geophysical survey data. *Period. Polytech. Civ. Eng.* **2018**, *62*, 893–900. [[CrossRef](#)]
19. Jordá-Bordehore, L. Application of Q slope to Assess the Stability of Rock Slopes in Madrid Province, Spain. *Rock Mech. Rock Eng.* **2017**, *50*, 1947–1957. [[CrossRef](#)]
20. Wyllie, D.C.; Mah, C.W. Rock slope engineering: Civil and mining. In *Rock Slope Engineering*, 4th ed.; CRC Press: London, UK, 2017. [[CrossRef](#)]
21. Hoek, E.; Bray, J. *Rock Slope Engineering*, 3rd ed.; Institution of Mining and Metallurgy: London, UK, 1981.
22. Jorda, L.; Tomás, R.; Rodríguez, M.A.; Abellan, A. *Manual de Estaciones Geomecánicas*; Universidad Politécnica de Madrid: Madrid, Spain, 2016; p. 208.
23. UNESCO. Galapagos Biosphere Reserve, Ecuador. 1976. Available online: <https://en.unesco.org/biosphere/lac/galapagos> (accessed on 16 July 2022).
24. Wolf, T. *Geografía y Geología de Ecuador*; Brockhaus, F.A., Ed.; Leipzig: Alicante, Spain, 1892. Available online: <http://files.bernardo-servin-massieu.com/200000059-af10bb00a5/tabasco.pdf> (accessed on 10 January 2021).
25. Jordá-Bordehore, L.; Tomás, R.; Cano, M.; Riquelme, A. Evaluación de la calidad geomecánica de taludes inestables en la zona andina mediante la aplicación de la clasificación Slope Mass Rating. In Proceedings of the 10° Simposio Nacional de Ingeniería Geotécnica, A Coruña, España, 19–21 October 2016; Volume 1, pp. 313–320. Available online: https://www.researchgate.net/publication/309611438_Evaluacion_de_la_calidad_geomecanica_de_taludes_inestables_en_la_zona_andina_mediante_la_aplicacion_de_la_clasificacion_Slope_Mass_Rating (accessed on 29 January 2021).
26. Barton, N. Some new Q-value correlations to assist in site characterisation and tunnel design. *Int. J. Rock Mech. Min. Sci.* **2002**, *39*, 185–216. [[CrossRef](#)]
27. Barton, N.; Grimstad, E. Tunnel and cavern support selection in Norway, based on rock mass classification with the Q-system. *Nor. Tunn. Soc.* **2014**, *23*, 39. Available online: https://www.researchgate.net/publication/321874893_Tunnel_and_cavern_support_selection_in_Norway_based_on_rock_mass_classification_with_the_Q-system (accessed on 29 January 2021).
28. Bar, N.; Barton, N.R.; Ryan, C.A. Application of the Q-slope method to highly weathered and saprolitic rocks in Far North Queensland. In Proceedings of the ISRM International Symposium—EUROCK, Ürgüp, Turkey, 29–31 August 2016; Volume 1, pp. 585–590. [[CrossRef](#)]
29. Rocscience. 2D and 3D Geotechnical Software | Rocscience Inc. 2019. Available online: <https://www.rocscience.com> (accessed on 15 June 2021).
30. Mikola. Roozbeh Gerail Mikola—Codes & Demos. 2018. Available online: <http://www.roozbehgm.com/codes.html> (accessed on 20 September 2022).
31. Visa, S.; Ramsay, B.; Ralescu, A.L.; Van Der Knaap, E. Confusion Matrix-based Feature Selection. In Proceedings of the 22nd Midwest Artificial Intelligence and Cognitive Science Conference 2011, Cincinnati, OH, USA, 16–17 April 2014. Available online: https://www.researchgate.net/publication/220833270_Confusion_Matrix-based_Feature_Selection (accessed on 19 July 2022).
32. Beauxis-Aussalet, E.H.L. Simplifying the Visualization of Confusion Matrix. In Proceedings of the BNAIC—Benelux Conference on Artificial Intelligence, Nijmegen, The Netherlands, 6–7 November 2014. Available online: https://www.researchgate.net/publication/302412429_Simplifying_the_Visualization_of_Confusion_Matrix (accessed on 17 July 2022).
33. Stehman, S.V. Selecting and Interpreting Measures of Thematic Classification Accuracy. *Remote Sens. Environ.* **1997**, *62*, 77–89. Available online: <https://www.sciencedirect.com/science/article/pii/S0034425797000837> (accessed on 20 September 2022). [[CrossRef](#)]
34. Yacouby, R.; Axman, D. Probabilistic Extension of Precision, Recall, and F1 Score for More Thorough Evaluation of Classification Models. In Proceedings of the First Workshop on Evaluation and Comparison of NLP Systems 2020, Online, November 2020; pp. 79–91.
35. Hoek, E. Putting numbers to geology—An engineer’s viewpoint. *Q. J. Eng. Geol.* **1999**, *32*, 283–293. [[CrossRef](#)]

Disclaimer/Publisher’s Note: The statements, opinions and data contained in all publications are solely those of the individual author(s) and contributor(s) and not of MDPI and/or the editor(s). MDPI and/or the editor(s) disclaim responsibility for any injury to people or property resulting from any ideas, methods, instructions or products referred to in the content.